Influence Of Additional Attenuation Of Small Strain Shear Modulus G_{max} On Site Seismic Response

B. Huang, L. Li, D. S. Ling & M. X. Shi
Zhejiang University, China

SUMMARY:
Small strain shear modulus G_{max} is an important parameter in the site seismic response analysis. To access the progressive liquefaction phenomenon, the change of dynamic properties of shear modulus, G_{max} and G due to pore-water pressure increasing are always considered in seismic response analyses of saturated horizontal sand deposits. Hardin formula is often adopted to calculate G_{max}, but which has not considered the influence of an important factor, cyclic vibrating history. The effect of cyclic history on G_{max} has been examined by lots of dynamic triaxial tests on kinds of soils with measurement of shear wave velocities, from which we can deduce G_{max} after vibration. A refined one-dimensional equivalent linearization method has been proposed on the basis of effective stress principle, to account for the influence of additional attenuation of G_{max} associated with site seismic response. The comparison of site response with and without considering of the seismic history on G_{max} is also included.

Keywords: Small strain shear modulus; Additional attenuation; Site seismic response; Effective stress analysis method; Bender element

1. INTRODUCTION

As we all known, earthquake is an event which people can hardly control, and this reason makes it very important to study the earthquake. In the field of geotechnical earthquake engineering, the earthquake response on free sites is always the basement of seismic studies.

Small strain shear modulus G_{max} is an important parameter in the site seismic response analysis. Currently the site seismic response analysis usually use the effective stress method which can consider the pore pressure increase and effective stress decrease during earthquake shaking. According to G_{max} and the relation of G/G_{max} versus shear strain, the shear modulus G of soil can be got. Then G is used in dynamic equation to compute the response quantities such as acceleration, velocity, displacement and stress, strain and pore pressure and so on. This process is actually the so-called site seismic response analysis.

The most common used equation to calculate G_{max} is proposed by Hardin and his colleagues, where Hardin and Blandford (1989) finally summarized the expression as

$$G_{max}^{ij} = OCR^k \cdot F(e)\frac{S_{ij}P_a^{(1-n)}}{2(1+\nu)}(\sigma_i'\sigma_j')^{n/2} \tag{1.1}$$

in which G_{max}^{ij} is the initial shear modulus of plane ij; OCR is overconsolidation ratio; k has a relationship with the plasticity index, and for cohesionless soil can be considered as zero; $F(e)=1/(0.3+0.7e^2)$, in which e is porosity; S_{ij} is the elastic rigidity coefficient of plane ij, and dimensionless; P_a is the atmospheric pressure; ν is Poisson ratio; σ_i' is the effective stress in particle movement direction; σ_j' is the effective stress in wave propagation direction; and n is experimental constant. The expression gives a quantitative correlation of G_{max} and effective stress, void ratio and soil stress history.

Whereas, many researches have demonstrated that G_{max} is not only affected by the above factors, but also influenced by vibrating history. But few people considered the influence of earthquake history on site seismic response. This article summarizes previous researches of the influence of cyclic vibrating history on G_{max}, and developed a one-dimensional effective stress analysis procedure to take influence of the additional attenuation of G_{max} on site response analysis into account. The results show that the additional attenuation of G_{max} makes an advanced liquefaction in a liquefiable site.

2. PREVIOUS STUDY OF INFLUENCE OF CYCLIC VIBRATING HISTORY ON G_{max}

2.1. Influence of Small Amplitudes of Cyclic Vibrating History on G_{max}

Previous studies indicate that cyclic loading can change the number, orientation and shape of particle contacts as well as the distribution of interparticle forces in soil mass, therefore has an influence on small strain dynamic characteristics. Drnevich and Richard (1970) studied the influence of torsion shear vibration history on shear modulus and damping ratio of hollow cylinder samples in the resonant column device. The tests were performed on dry medium sands, and results showed that larger previbration would change the subsequent small strain dynamic characteristics of specimens. When the specimen had experienced 22 million cycles of vibration, the G_{max} measured after reconsolidation could even be larger than the G_{max} measured on the same static state but without previbration maximally by three times. Shen et al. (1985) used a microcomputer based free torsional vibration testing system to study the influence of number of cyclic vibration and initial shear strain on G_{max} of the dense and loose sands. The values of G_{max} were found increased for the increased number of cyclic vibration, and after 50,000 cycles of vibration the increase of G_{max} were in the range of 80% for the loose sands and in the range of 35% for the dense sands. Moreover, the increase of initial shear strain made the decrease of G_{max} of sands, and which situation was more obvious for dense sands than loose sands. Alarcon et al. (1989) used a testing device with integrated resonant column and torsional shear mode to study the influence of cyclic vibration history on G_{max} of dry coarse sand. They found a moderate increase (approximately 5%) of G_{max} due to previbrating for a large number of cycles with the amplitude of shear strain being 1.3×10^{-4}. However, they supposed the moderate increase of G_{max} was caused by the change of void ratio. Thus, small strain shear modulus G_{max} was considered to be insensitive to cyclic vibrating history. After series of experimental researches, Lo Presti et al. (1993) and Li et al. (1998) proposed a so-called threshold value of amplitude of preshearing strain, which was generally on the scale of 10^{-4}. They observed that preshearing strain with amplitudes lower than the threshold value has no significant effect on G_{max} and damping ratio. When amplitudes of preshearing strain exceeded the threshold value, G_{max} would decrease or increase slightly as the number of preshearing cycles increased, but damping ratio would decrease substantially, and lager amplitudes of preshearing strain could make lager decreases of damping ratio.

2.2. Influence of Large Amplitudes of Cyclic Vibrating History on G_{max}

Formally, measurements of dynamic shear modulus G and small strain shear modulus G_{max} in laboratory tests were mainly conducted using resonant column or torsion shear apparatus and so on. For the limitation of instrument properties, amplitudes of vibrating strain could hardly be larger than 10^{-3}. On these situations of small amplitudes of strain and very high numbers of vibrating, specimens suffered equivalently from forces of long-term and small amplitudes of vibrating history. Actually, an earthquake (generally means principal earthquake) only lasts for seconds, but in such a short time, it can make the soil generate large deformation and cause the pore pressure growth, or even liquefaction. In order to simulate these features, samples in laboratory testing should suffered large amplitude but short time cyclic vibrations.

In recent years the bender element test has become an important means to measure G_{max}. Within the bender element in the dynamic triaxial apparatus, one can possibly study the influence of cyclic vibrating on G_{max} under situations similar to real earthquake.

Wichtmann and Triantafyllidis (2004) conducted series of cyclic preloading tests on dry sand samples affected by the average state of stress, initial relative density, amplitude of cyclic loading and category of particle separately using triaxial apparatus installed with bender element. They finally detected no significant influence of the above factors on G_{max}, and G_{max} generally changed in the range of 0.9~1.1G_{max0} (G_{max0} was the small strain shear modulus of samples on the same states but without cyclic preloading history).

Ji Meixiu (2005), Zhou and Chen (2005), Zhang Jun (2006) and Shi Mingxiong (2008) conducted series of laboratory experiments to research the influence of large amplitudes of cyclic vibrating history on G_{max} on different kinds of saturated soils using the dynamic triaxial apparatus with piezoelectric-ceramic bender elements. Through the tests they found that except the decrease of G_{max} as pore pressure increase and effective stress decrease as we all have known, there is still 0~50% attenuation, which can be called the additional attenuation of G_{max}.

Summaries for different soil types, different dense degrees, different vibrating ways concluded by each researcher are shown in Table 2.1.

Table 2.1. Summary Of Influences Of Cyclic Vibrating History On G_{max}

Researcher	Soil type	Dense degree	Vibrating way	Conclusion
Ji Meixiu	Sand	Medium and dense	Unidirectional	G_{max} values measured under dynamic and static states are similar for the same effective stress.
	Undisturbed silt	Low liquid limit silt		If dynamic strain is less than the threshold strain, conclusion is the same as above. If dynamic strain is greater than the threshold strain, G_{max} measured under dynamic state is less than that measured in static state for the same effective stress.
	Undisturbed marine clay	Low liquid limit clay		Conclusion is the same as silt.
Zhou and Chen	Sand	Medium and Fine	Unidirectional	G_{max} measured under dynamic state is less than that measured in static state for the same effective stress, which degree for medium sands can be 6%~9%, and for fine sands can be 3%~5%.
Zhang Jun	Silt	Medium and dense	Unidirectional	Additional attenuations happen to G_{max} influenced by different cyclic shear stress ratios, relative densities and initial small strain shear modulus, but in some cases G_{max} can also be strengthened.
Shi Mingxiong	Sand	Medium and loose	Unidirectional and bidirectional	When effective stress ratio σ'_c/σ'_{c0} decreases to 0.6~0.65, obvious additional attenuations of G_{max} begin to happen, and the maximum additional attenuation rate can be 20% while σ'_c/σ'_{c0}=0.4. Moreover different vibrating ways have no significant effects on conclusions.
	Silt	Dense, medium and loose	Unidirectional	Additional attenuations of G_{max} for dense samples are small, approximately within 3%. For medium samples additional attenuations are very obvious after some cycles of dynamic loading, maximally can be 50%. Obvious additional attenuations of G_{max} for loose samples happen at the beginning, and reach to the maximum 9~14% while σ'_c/σ'_{c0}=0.3.

No matter for sand, silt or clay, there all exist the phenomenon of additional attenuation of G_{max}. However, the modes of additional attenuation for different types of soil are different with the factors, such as relative densities, cyclic shear stress ratios and so on. The reason for the additional attenuations of G_{max} is thought to be the particles slipping and changes of interparticle forces in the shaking.

Fig. 2.1 gives some typical curves which show the additional attenuations of G_{max}. The dotted lines express fitted curves for Hardin formula in static states, and the discrete points are G_{max} data measured under dynamic states after normalization. Through the comparison of the dotted line and discrete points in each figure, we can find out that discrete points are mainly beneath the dotted line, which show the phenomenon of additional attenuation of G_{max}.

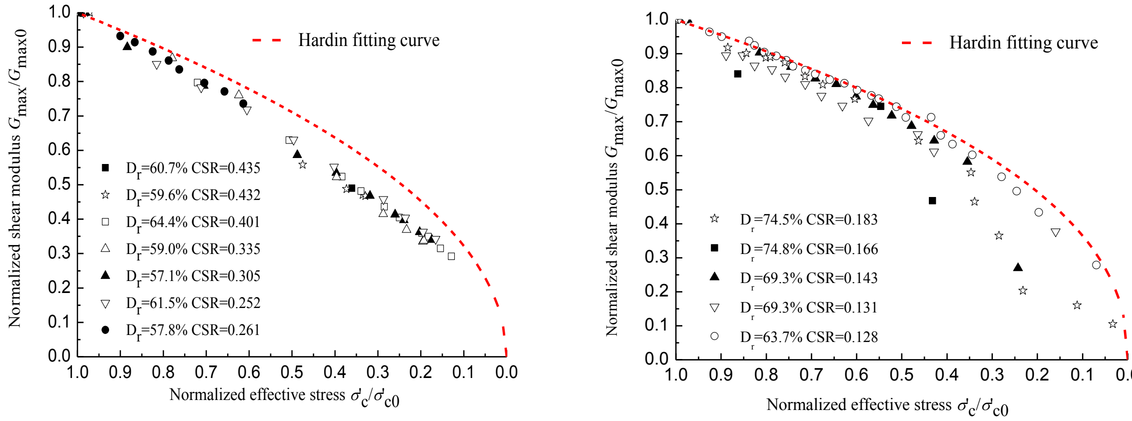

(a) Medium dense sand specimen (b) Dense silt specimen

Figure 2.1. Relations for G_{max}/G_{max0} versus σ_c'/σ_{c0}'

3. SITE SEISMIC ANALYSIS MODEL TO CONSIDER THE INFLUENCE OF ADDITIONAL ATTENUATION OF G_{max}

A refined one-dimensional equivalent linearization method has been proposed on the basis of effective stress principle, to account for the influence of additional attenuation of G_{max} associated with site seismic response. The stratum is regarded as a one-dimensional shear beam, and the shear beam is represented by a lumped mass model.

The dynamic equation of motion of the lumped mass system is given by

$$[M]\{\ddot{u}\}+[C]\{\dot{u}\}+[K]\{u\}=0 \tag{3.1}$$

in which [M] = total mass matrix; [C] = total damping matrix; [K] = total stiffness matrix; and $\{\ddot{u}\}$, $\{\dot{u}\}$, and $\{u\}$ = the absolute acceleration, velocity and displacements of the masses. The mass matrix [M] and stiffness matrix [K] are determined based on the lumped mass model; Rayleigh damping is applied to the model which is expressed as $[C^e]=\alpha[M^e]+\beta[K^e]$, where $[M^e]$,$[K^e]$ = the unit mass matrix and unit stiffness matrix; $\alpha=\lambda\omega$ and $\beta=\lambda/\omega$, in which λ = the damping coefficient of the unit and ω = the fundamental circular frequency of the system. To solve Eqn. 3.1, a direct numerical integration method, Newmark-beta method, is used.

To take it into account that the pore pressure of soil increases and effective stress decreases during seismic process, the duration time of earthquake should be divided into several short time intervals and dynamic analysis is done in each time internal. The flow chart of the computational process is shown in Fig. 3.1.

To solve Eqn. 3.1 during a time interval, the shear modulus G is required. Meanwhile the G_{max}, the relation of $G/G_{max}\sim\gamma$ (Fig. 3.2) and the shear strain γ are necessary to get G. What deserves to be mentioned is that, the forms of $G/G_{max}\sim\gamma$ in each time intervals are identical. When one interval time ends, due to the pore pressure increase and effective stress decrease a new G_{max} is got for next time interval use. Previously the methods to calculate G_{max} based on effective stress didn't consider the influence of cyclic vibrating history. However in this progress, G_{max} can be calculated considering the influence of cyclic vibrating history. To calculate G_{max}, the initial G_{max0} and the relations of $G_{max}/G_{max0} \sim \sigma'_c / \sigma'_{c0}$ (see Fig. 2.1) are required.

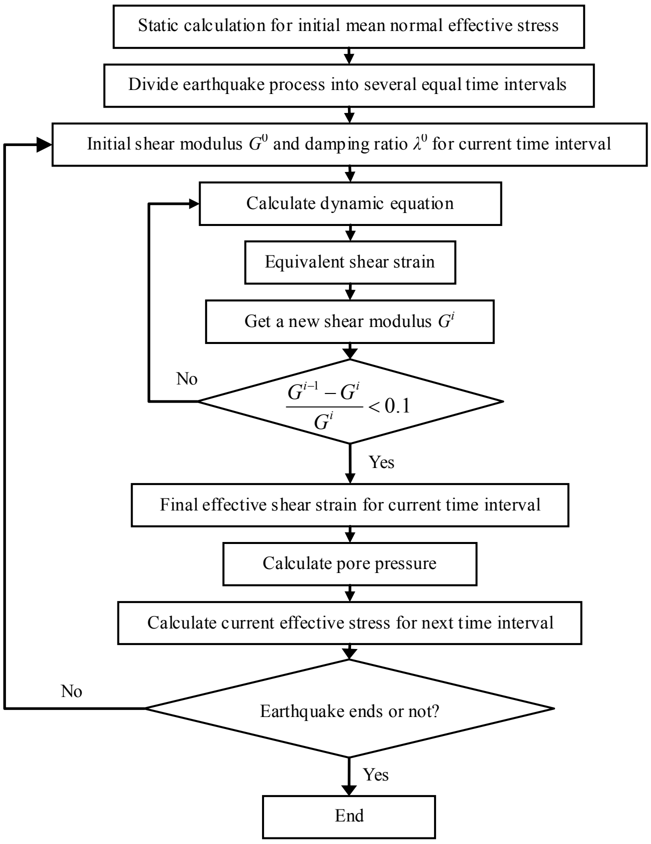

Figure 3.1. Flow chart of computational procedure

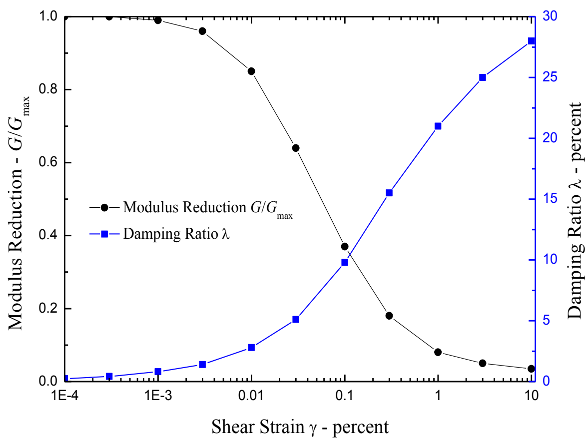

Figure 3.2. Relations for G/G_{max} and damping ratio versus shear strain

The expression to calculate the initial G_{max0} used in the program is

$$G_{\max 0} = 6920 K_2 (\sigma'_{c0})^{1/2} \tag{3.2}$$

in which σ'_{c0} is the initial mean effective stress; $K_2 = 43$ according to the literature (Finn et al. 1976).

SI is used in this equation.

The development of pore pressure is the same as which Finn proposed (Finn et al. 1976). The equation to calculate the rise in pore-water pressure Δu, during a cycle of shear strain γ, is as

$$\Delta u = \bar{E}_r \Delta\varepsilon_{vd} \tag{3.3}$$

in which $\Delta\varepsilon_{vd} = C_1(\gamma - C_2\varepsilon_{vd}) + \frac{C_3\varepsilon_{vd}^2}{\gamma + C_4\varepsilon_{vd}}$ is the volumetric strain increment; $\bar{E}_r = \frac{(\sigma_v')^{1-m}}{mk_2(\sigma_{v0}')^{n-m}}$ is the one-dimensional rebound modulus; ε_{vd} is the total accumulated volumetric strain; σ_{v0}' is the initial vertical effective stress while σ_v' is the current vertical effective stress; C_1, C_2, C_3, C_4, m, n, k_2 are all experimental parameters.

4. EXAMPLES

4.1. Site Conditions and Parameter Selected

Using what described above, the authors compiled a program to analysis the influence of the additional attenuation of G_{max} on seismic response of the free site. The site is horizontal, composed with homogeneous sand, 15m depth. The water table lies on the ground surface. The unit weight of the sand is $18kN/m^3$.

The site is divided into 10 layers so that the thickness of each layer is 1.5m. In the procedure, it uses the initial G_{max0} and the relation of $G_{max}/G_{max0} \sim \sigma_c' / \sigma_{c0}'$ in Fig. 2.1(a) to computer G_{max} based on the current mean effective stress σ_c'. The Fig. 2.1(a) consists two kinds of situations with and without considering the additional attenuation of G_{max} as which have been stated. The soil parameters for calculating Eqn.3.3 are taken identical to which Finn provided (Finn et al. 1976).

The input waves are separately sinusoidal wave with a frequency of 2Hz and El-Centro wave with a maximum acceleration of 0.1g. The duration times are both 10s. Moreover, the responses based on the effective stress method with and without the consideration of additional attenuation of G_{max} are compared for both inputs.

4.2. Site Seismic Response to Sinusoidal Wave Input

A sinusoidal wave with a maximum acceleration of 0.04g is used to input. The surface accelerations computed with and without considering additional attenuation of G_{max} show different response histories in Fig. 4.1. In the case of not considering the additional attenuation of G_{max}, the accelerations gradually increase and then decrease to effectively zero after about 6.5s. While in the case of considering the additional attenuation of G_{max}, it is at about 3s when the accelerations decrease to zero. The pore pressure development in top layer (Fig. 4.2) shows that the pore pressures increase at a faster rate to the initial effective stress when considering the additional attenuation of G_{max}. So the site liquefies in both cases and for the case of considering the additional attenuation of G_{max} the site liquefies sooner than that not considering additional attenuation. It can also be concluded that the model used to consider the additional attenuation of G_{max} doubles the speed of liquefaction while the maximum degree of additional attenuation is only 20%.

Fig. 4.3 shows the pore pressure distributions at 1s, 5s and final time in stratum for cases with and without considering the additional attenuation of G_{max}. It is clear that, no liquefaction appears at 1s and the pore pressures in two cases have no big differences. At 5s pore pressures rise and there are significant differences that no liquefaction happens in case of not considering the additional attenuation of G_{max} while some layers liquefies in case of considering the additional attenuation of

G_{max}. When shaking ends, the liquefaction depths of site are the same in both cases.

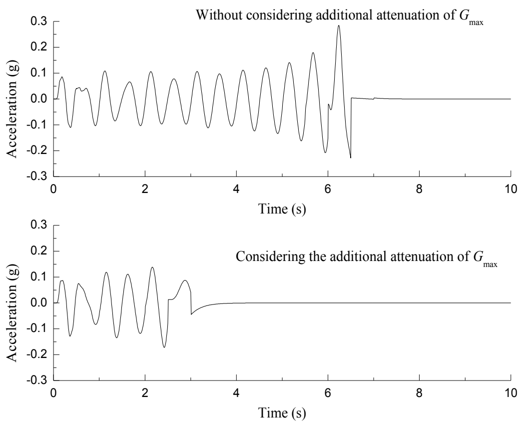

Figure 4.1. Surface accelerations computed with and without considering additional attenuation of G_{max}

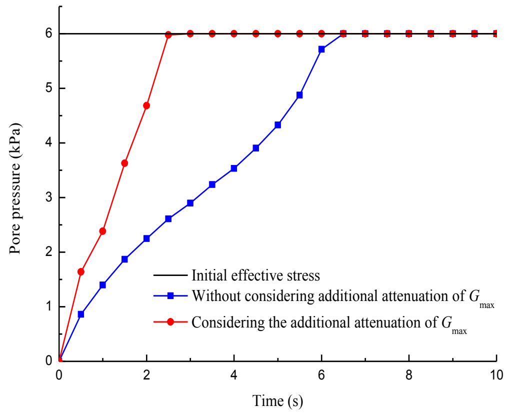

Figure 4.2. Pore pressure development in top layer for conditions with and without considering additional attenuation of G_{max}

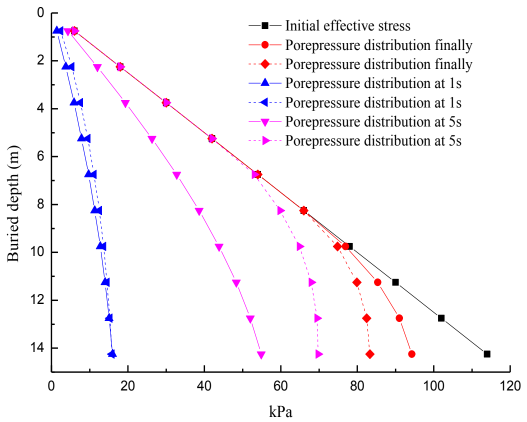

Figure 4.3. Pore pressure distribution in stratum

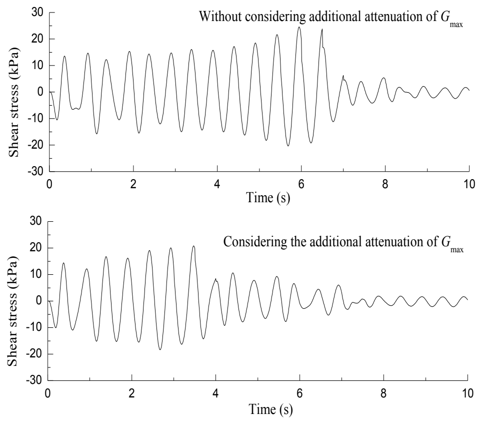

Figure 4.4. Shear strain time history in layer 7 for conditions with and without considering additional attenuation of G_{max}

However, the final pore pressures of non-liquefied layers in the case of not considering the additional attenuation of G_{max} are higher than that in the considering case. Which can be due to that the upper liquefied layers can not transfer forces and only the underneath non-liquefied layers bear forces in the whole system when the site liquefies, thus the shear shaking amplitudes of the non-liquefied layers decrease, and the shear stress amplitudes decrease, finally slowing down the increase of pore pressure. Consider the top layer to be the 1st layer, and so down. Fig. 4.4 shows the 7th layer (the top non-liquefied unit) shear stresses in two cases. The shear stresses gradually decrease after the liquefaction of site (at about 3s) in the case of considering the additional attenuation of G_{max}, while the shear stresses keep on increasing in the case of not considering the additional attenuation of G_{max} until its site liquefaction time (at about 6.5s). It just coincides with the above statement.

No matter for the conditions of considering or not considering additional attenuation of G_{max}, the site all liquefies in the above case of maximum input acceleration to be 0.04g. However, when the maximum input acceleration is used to be 0.03g, it can be found that no liquefaction happens in the case of not considering additional attenuation of G_{max} while there are 6.25m depth liquefaction of the site in the case of considering the additional attenuation of G_{max}, which can be seen in the final pore pressure distribution in stratum (Fig. 4.5).

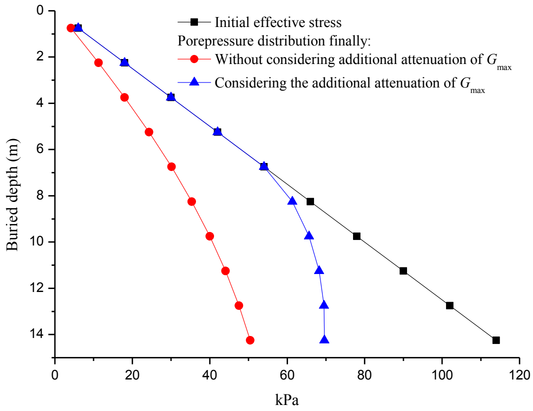

Figure 4.5. Final pore pressure distribution in stratum while input a_{max} = 0.03g

4.3. Site Seismic Response for El-Centro Wave Input Situation

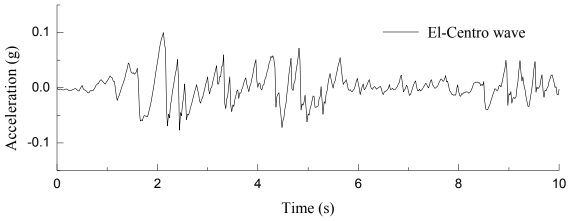

Figure 4.6. Input El-Centro wave

When the site suffers from El-Centro wave (Fig. 4.6), its seismic response results are shown in Fig. 4.7, Fig. 4.8 and Fig. 4.9. What can be seen in Fig. 4.7 and Fig. 4.8 are similar to the sinusoidal wave input case, the accelerations drop faster to zero and the pore pressures increase faster to the initial effective stress when considering additional attenuation of G_{max} than those do not consider the additional attenuation.

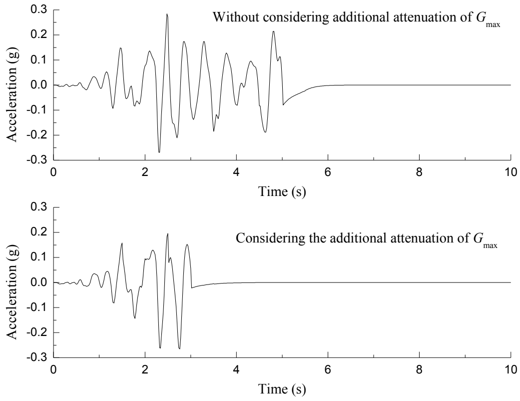

Figure 4.7. Accelerations at the top of layer 2 with and without considering additional attenuation of G_{max}

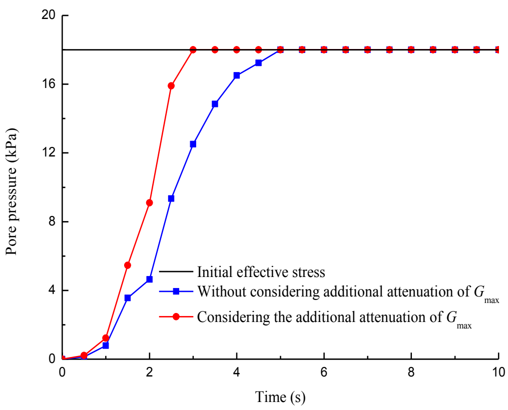

Figure 4.8. Pore pressure development in layer 2 for conditions with and without considering additional attenuation of G_{max}

Fig. 4.9 shows the pore pressure distributions at 1s, 3s and final time in stratum. At 1s, the pore pressures are very approximate in two cases and less than 5kPa. At 3s the pore pressures rise to 10-50kPa and the upper two layers liquefy in the case of considering additional attenuation of G_{max} while still no liquefaction happens in the case of not considering additional attenuation of G_{max}. However the pore pressures of some lower units are higher in the case of not considering additional attenuation of G_{max} than those in the case of considering additional attenuation of G_{max}, the reason for which is that liquefaction of upper layers can slow down the rise rate of pore pressures as explained in the sinusoidal wave input case. When the earthquake ends, the liquefaction depths are identical in both cases.

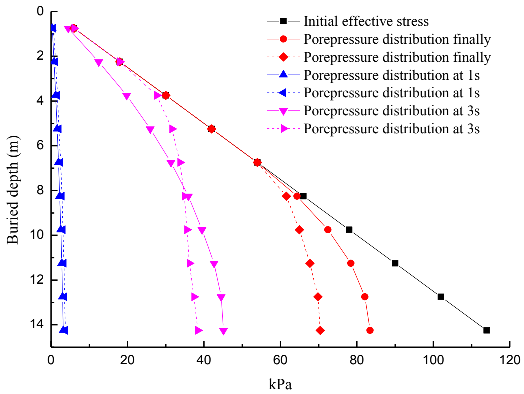

Figure 4.9. Pore pressure distribution in stratum

In conclusion, the influences of additional attenuation of G_{max} on site seismic response in the earthquake wave input case are similar to the sinusoidal wave case. The mainly influence is speeding up the site liquefaction, and which is thought due to that the additional attenuation of G_{max} makes the soil shear modulus decreases, and in the same effective stress state the soils soften faster to liquefaction. Moreover, not considering the additional attenuation of G_{max} may lead to liquefaction judgment faults.

5. CONCLUSIONS

Using the program compiled by authors to analyze the sand site seismic response under situations with and without considering the additional attenuation of G_{max} when the input wave is sinusoidal wave or El-Centro wave. Results all indicate that if considering the additional attenuation of G_{max}, the rise of pore pressure will be quicken, thus the liquefying time advances. The reason is considered to be that the additional attenuation of G_{max} makes the soil shear modulus decreases, so in the same effective stress state the soil softens faster to liquefaction.

However, the final pore pressures of non-liquefied layers in the case of considering the additional attenuation of G_{max} are less than those in the case of considering the additional attenuation of G_{max}. It can be due to that the upper liquefied layers can not transfer forces and only the underneath non-liquefied layers bear forces in the whole system when the site liquefies, thus the shear shaking amplitudes of the non-liquefied layers decrease, and the shear stress amplitudes decrease, finally slowing down the increase of pore pressure.

For large amplitudes input, both cases of considering and not considering the additional attenuation of G_{max} make the site liquefy. However for small amplitudes input, the site doesn't liquefy in the case of not considering the additional attenuation of G_{max} while some layers liquefy in the case of considering the additional attenuation of G_{max}. Thus, not considering the additional attenuation of G_{max} may lead to liquefaction judgment faults.

The analysis results show that the maximum of 20% additional attenuation of G_{max} can double the speed of liquefaction of sand site. So what can be concluded is that, if not considering the additional attenuation of G_{max}, the results of seismic response of silt sites may be very insecure because the additional attenuation of G_{max} of silt is more obvious than sand.

REFERENCES

Hardin, B. O. and Blandford, G. E. (1989). Elasticity of particulate materials. *Journal of Soil Mechanics and Foundations Division* **115:2**, 1449-1467.

Drnevich, V. P. and Richart, F. E. (1970). Dynamic prestraining of dry sand. *Journal of Soil Mechanics and Foundations Division* **96:2**, 453-467.

Shen, C. K., Li, X. S. and Gu, Y. Z. (1985). Microcomputer based free torsional vibration test. *Journal of Geotechnical Engineering* **111:8**, 971-986.

Alarcon-Guzman, A., Chameau, J. L., Leonardos, G. A. and Frost, J. D. (1989). Shear modulus and cyclic undrained behavior of sands. *Soils Foundations* **29:4**, 105-119.

Lo Presti, D. C. F., Pallara, O., Lancellotta, R., Armandi, M. and Maniscalco, R. (1993). Monotonic and cyclic loading behaviour of two sands at small strains. *Geotechnical Testing Journal* **16:4**, 409-424.

Li, X. S. and Yang, W. L. (1998). Effects of vibration history on modulus and damping of dry sand. *Journal Geotechnical and Geoenvironmental Engineering* **124:11**, 1071-1081.

Wichtmann, T. and Triantafyllidis, T. H. (2004). Influence of a cyclic and dynamic loading history on dynamic properties of dry sand, part I: cyclic and dynamic torsional prestraining. *Soil Dynamics and Earthquake Engineering* **24:2**, 127-147.

Wichtmann, T. and Triantafyllidis, T. H. (2004). Influence of a cyclic and dynamic loading history on dynamic properties of dry sand, part II: cyclic axial preloading. *Soil Dynamics and Earthquake Engineering* **24:11**, 789-803.

Ji, M. X. (2005). Study on the shear wave velocity measurement from bender elements and dynamic properties of saturated soft marine clay, Zhejiang University.

Zhou, Y. G. and Chen, Y. M. (2005). Influence of seismic cyclic loading history on small strain shear modulus of saturated sands. *Soil Dynamics and Earthquake Engineering* **25:5**, 341-355.

Zhang, J. (2006). Cyclic stress history effects on small strain shear modulus of silt, Zhejiang University.

Shi, M. X. (2008). Sand response to multi-way dynamic loading, Zhejiang University.

Finn, W. D. L., Byrne, P. M. and Martin, G. R. (1976). Seismic response and liquefaction of sand. *Journal of the Geotechnical Engineering Divison* **102:8**, 841-856.